

# Visible Light Emission from Slow Highly Charged Ions Transmitted Through a Ni Microcapillary

Yuichiro Morishita,<sup>1\*</sup> Shiro Ninomiya,<sup>1†</sup> Yasunori Yamazaki,<sup>1,4</sup> Ken-ichiro Komaki,<sup>1</sup> Kenro Kuroki,<sup>1</sup> Hideki Masuda<sup>2</sup> and Masayuki Sekiguchi<sup>3</sup>

<sup>1</sup> Institute of Physics, Graduate School of Arts and Sciences, University of Tokyo, Meguro, Tokyo 153-8902, Japan

<sup>2</sup> Department of Industrial Chemistry, Faculty of Engineering, Tokyo Metropolitan University, Hachioji, Tokyo 192-0397, Japan

<sup>3</sup> Center for Nuclear Study, School of Science, University of Tokyo, Tanashi, Tokyo 188-0002, Japan

<sup>4</sup> RIKEN, Wako, Saitama 351-0198, Japan

Received September 14, 1998; accepted in revised form December 3, 1998

PACS Ref: 3450Dy

## Abstract

Interaction of slow highly charged ions (HCI) with a thin microcapillary foil was studied for the first time through measurements of visible light emitted from the ions downstream of the foil. The microcapillary was employed so that ions which capture electrons in high Rydberg states may not violently collide with the surface in spite of the image acceleration. The wavelength range measured was from 300 nm to 600 nm. Some strong lines were found attributable to  $\Delta n = 1$  transitions resulting from a single electron capture into states with  $n_i \sim Q$  and with a large angular momentum.

## 1. Introduction

Recently the interactions of slow HCIs with surfaces [1] and atoms [2] have been studied intensively through measurements of energy distributions of Auger electrons, X-rays and scattered ions. In the HCI-atom collision experiments, visible light measurements have also been done [3].

According to the classical over-barrier model (COBM) [4], when a slow HCI approaches a surface, electrons near the Fermi level of the solid start to be resonantly transferred to the HCI at a critical distance  $d_c = \sqrt{2Q}/W$ , where  $Q$  is the charge state of the ion and  $W$  is the workfunction of the solid. The principal quantum number  $n_c$  in which electrons are captured at the beginning is  $n_c \simeq Q/\sqrt{2W(1 + (Q - \frac{1}{2})/\sqrt{8Q})}$ . The HCI is accelerated towards the surface by the self image force, and captures electrons successively in the lower states, and then violently collides with the surface. For example, in the case of a  $\text{Ar}^{8+}$  incident on a Ni surface ( $W \sim 5$  eV),  $d_c$  and  $n_c$  are about 22 a.u. and 9, respectively. The time interval between  $d = d_c$  and  $d = 0$  is about  $10^{-14} \sim 10^{-13}$  s at the longest, where  $d$  is the distance between the ion and the surface. As a typical radiative lifetime in the visible light region is of the order of ns, there are few chances for the ion to be de-excited through the visible light emission. This may be the principal reason why spectroscopic experiments in the visible light range have not been performed in HCI-surface collisions.

In order to avoid the above-mentioned difficulty, we have used a so-called microcapillary target made of Ni. In the previous study [5], we succeeded in extracting stabilized hollow atoms (ions) in the vacuum, which was confirmed by lifetime

measurements of X-rays emitted from the ions. In this paper, we report the microcapillary experiments extended to the visible light region for the first time.

## 2. Experiment

The experimental set up is drawn in Fig. 1. The 14 GHz HyperECR ion source at the Center for Nuclear Study, University of Tokyo was used to produce multiply charged ions of  $\text{Ar}^{Q+}$  ( $8 \leq Q \leq 11$ ). Extracted Ar ions were accelerated to 10Q keV, charge-state analyzed by a magnet, collimated by four-jaw slits, and then transported to a Ni microcapillary target in a vacuum chamber. The pressure of the chamber was kept below  $1 \times 10^{-8}$  Torr during the measurements. The target was installed on a manipulator which was movable in three translational and two rotational directions. The thickness and the hole diameter of the target were about 1.5  $\mu\text{m}$  and 250 nm, respectively. A lens partially hidden by a slit was placed on a direction perpendicular to the beam axis to collect photons emitted from the Ar ions downstream of the target. The photons were guided via an optical fiber to a monochromator of 500 mm focal length (Acton SP500) which had a grating of 1200 grooves/mm and 300 nm blaze wavelength. The dispersed light was detected by a photomultiplier (Hamamatsu R2757). A mercury lamp was used for wavelength calibration, and a standard tungsten lamp was used for relative intensity calibration.

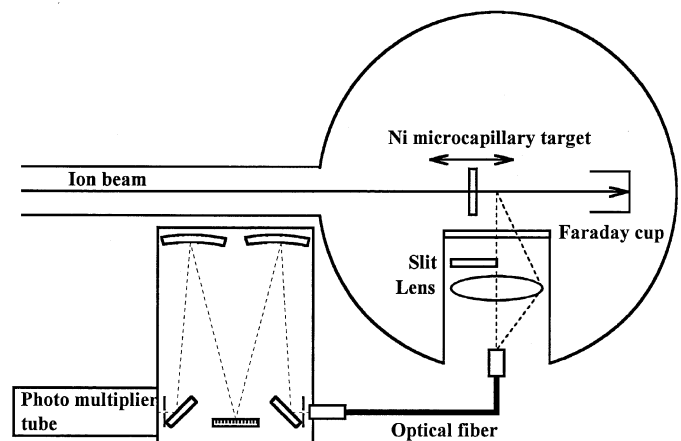


Fig. 1. Experimental setup.

\* e-mail: morisita@radphys4.c.u-tokyo.ac.jp

† Present address: Research Center for Nuclear Physics, Osaka University, Ibaraki, Osaka 567-0047, Japan

### 3. Results and discussion

Observed spectra for  $10Q$  keV  $\text{Ar}^{Q+}$  ( $8 \leq Q \leq 11$ ) incidences on the microcapillary are shown in Fig. 2. These spectra are calibrated absolutely in wavelength and relatively in intensity. The spectral resolutions in these observations are about 2.3 nm for  $\text{Ar}^{8+}$  and  $\text{Ar}^{9+}$  incidences, and 4.5 nm for  $\text{Ar}^{10+}$  and  $\text{Ar}^{11+}$  incidences. The broad peak around 350 nm is seen for all spectra and consists of many sharp peaks in a high resolution measurement which can be attributed to transitions of the sputtered Ni atoms [6]. The rest of the peaks originate from the transitions of Ar ions. The observed peaks are listed in Table I. The values of wavelength and its error were obtained in measurements with higher resolution. The COWAN code [7] based on the multiconfiguration Hartree-Fock method was used to identify each transition. The calculations were performed for  $\text{Ar}^{Q+}$  ( $Q = 8, 9$  and  $10$ ) incidences, assuming that the incident ions are in the ground states and one electron is captured in high Rydberg states, and the ions decay through  $\Delta n = 1$  transitions. As an example, the result of the calculation for  $\text{Ar}^{8+}$  is shown in Table II. By comparing observed and calculated values, it is concluded that the peak referred to as *a* in Fig. 1 can be attributed to  $9l - 8l'$  transitions with  $l, l' \geq 5$ . Such large angular momenta may be explained by an extended COBM [8]. In the same way, peaks referred to as *b*, *c* and *d* can be attributed to one electron captures in high Rydberg states (Table I). Because the incident ions have L-shell holes, which makes the electronic configurations complicated, and the spectral resolution was lower than that of  $\text{Ar}^{8+}$  incidence, the angular momenta could not be determined as precisely as in the case of  $\text{Ar}^{8+}$  incidence. For  $\text{Ar}^{11+}$  incidence, the transition corresponding to the peak *e* was deduced by employing the formula  $E_n = -(Q^2/2n^2)$ .

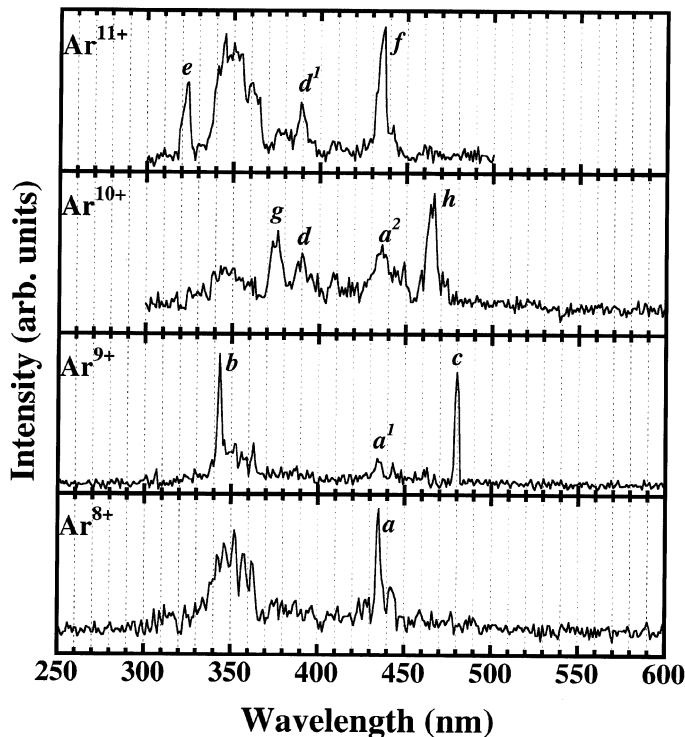


Fig. 2. Observed spectra for  $10Q$  keV  $\text{Ar}^{Q+}$  ( $8 \leq Q \leq 11$ ) incident through the Ni microcapillary.

Table I Observed peak wavelengths and their identifications. Transitions which can not be identified are indicated as "unknown".

Incident energy	Incident energy (keV)	Wavelength (nm)	Transition
$\text{Ar}^{8+}$	80	a	$9l - 8l', l, l' \geq 5$
$\text{Ar}^{9+}$	90	b	$9l - 8l', l, l' \geq 3$
		$a^1$	$\text{Ar}^{8+}; 9l - 8l' ?$
		c	$10l - 9l', l, l' \geq 3$
$\text{Ar}^{10+}$	100	g	unknown
		d	$10l - 9l', l, l' \geq 2$
		$a^2$	$\text{Ar}^{8+}; 9l - 8l' ?$
		h	unknown
$\text{Ar}^{11+}$	110	e	$10l - 9l'$
		$d^1$	$\text{Ar}^{10+}; 10l - 9l' ?$
		f	$\frac{11l - 10l'}{\text{Ar}^{8+}; 9l - 8l' ?}$

Table II Possible transitions around the peak *a* ( $434.3 \pm 0.5$  nm). It is seen that the transitions from  $1s^2 2s^2 2p^6 9l$  states to  $1s^2 2s^2 2p^6 8l'$  states ( $l, l' \geq 5$ ) are the candidates.

Upper configuration	Lower configuration	Transition wavelength (nm)
$9f^1 \ ^2F_{7/2,5/2}$	$8d^1 \ ^2D_{5/2,3/2}$	392.6, 392.6, 392.4
$9f^1 \ ^2F_{7/2,5/2}$	$8g^1 \ ^2G_{9/2,7/2}$	436.7, 436.7, 436.7
$9g^1 \ ^2G_{9/2,7/2}$	$8f^1 \ ^2F_{7/2,5/2}$	429.4, 429.4, 429.4
$9g^1 \ ^2G_{9/2,7/2}$	$8h^1 \ ^2H_{11/2,9/2}$	435.1, 435.1, 435.1
$9h^1 \ ^2H_{11/2,9/2}$	$8g^1 \ ^2G_{9/2,7/2}$	432.7, 432.7, 432.6
$9h^1 \ ^2H_{11/2,9/2}$	$8i^1 \ ^2I_{13/2,11/2}$	434.5, 434.5, 434.4
$9i^1 \ ^2I_{13/2,11/2}$	$8h^1 \ ^2H_{11/2,9/2}$	433.9, 433.8, 433.8
$9i^1 \ ^2I_{13/2,11/2}$	$8k^1 \ ^2K_{15/2,13/2}$	434.2, 434.2, 434.2
$9k^1 \ ^2K_{15/2,13/2}$	$8i^1 \ ^2I_{13/2,11/2}$	434.2, 434.1, 434.1
$9l^1 \ ^2L_{17/2,15/2}$	$8k^1 \ ^2K_{15/2,13/2}$	434.2, 434.2, 434.2

It is noted that there are peaks which can not be reasonably attributed to one electron capture in high Rydberg states. What is characteristic of some of them is that peaks  $a^1$  and  $a^2$  have, in the present spectral resolution, almost the same wavelength as the peak *a*, and the peak  $d^1$  has the same wavelength as the peak *d*. This may indicate that the charge states of the ionic cores are  $\text{Ar}^{8+}$  for  $a^1$  and  $a^2$ , and  $\text{Ar}^{10+}$  for  $d^1$  at the moment of the transitions. Since the decay rate via auto-ionization is generally larger than that via radiation, this fact may be understood in terms of auto-ionization after multiple electron capture. The peak *f* can be understood in two ways. If one electron capture is considered, the transition energy from  $11l$  to  $10l'$  is calculated to be 434.7 nm by using the above formula. And since the wavelength of the peak *f* has almost the same value as that of the peak *a*, the peak *f* can be explained as a result of multiple electron capture. But in the present resolution, it is difficult to say whether this originates from one electron capture, multiple electron capture, or both.

### 4. Summary

Visible light emissions from HCIs which result from the interaction with a metal surface were measured for the first time. For all charge states measured ( $8 \leq Q \leq 11$ ), photon emissions due to one electron capture were observed. Photon emissions that may result from multiple electron capture were also observed.

**References**

1. Meyer, F.W. *et al.*, Phys. Rev. Lett. **67**, 723 (1991); Briadn, J. P. *et al.*, Phys. Rev. Lett. **65**, 159 (1990); Winter, H., Europhys. Lett. **18**, 207 (1992).
2. Bordenave-Montesquieu, A. *et al.*, J. Phys. B: At. Mol. Phys. **17**, L223 (1984); Bliman, S. *et al.*, J. Phys. B: At. Mol. Phys. **25**, 2065 (1992); Tsurubuchi, S. *et al.*, J. Phys. B: At. Mol. Phys. **15**, L733 (1982).
3. Jacquet, E. *et al.*, Physica Scripta **47**, 618 (1993).
4. Burgdoerfer, J., Lerner, P. and Meyer, F.W., Phys. Rev. A **44**, 5674 (1991).
5. Ninomiya, S. *et al.*, Phys. Rev. Lett. **78**, 4557 (1997).
6. Tolk, N. H., Simms, D. L., Foley, E. B. and White, C.W., Radiation Effects **18**, 221 (1973).
7. Cowan, R. D., "The Theory of Atomic Structure and Spectra" (University of California Press, Berkeley, 1981).
8. Burgdoerfer, J., Morgenstern, R. and Niehaus, A., J. Phys. B: At. Mol. Phys. **19**, L507 (1986).